CHAPTER 1

Introduction

1.1 The interstellar medium

Our Galaxy is largely empty. By terrestrial standards the space between the stars can be considered as a near-perfect vacuum: the average particle density in the solar neighborhood is roughly a factor of 10^{19} less than in the terrestrial atmosphere at sea level. However, the highly diluted material present between the stars, the so-called InterStellar Medium (ISM), plays a central role in the chemical evolution of the Galaxy. The ISM is the repository of ashes from previous generations of stars and it is itself the birthplace of new stars and planetary systems. The interstellar matter consists of about 99% gas and 1% (sub)micron size silicate and carbonaceous dust grains by mass. The interstellar gas is composed of roughly 89% hydrogen, 9% helium and 2% heavier elements. The gas in the ISM is found in a variety of phases: coronal gas, ionized gas, neutral atomic gas and molecular gas (Tielens 2005). The physical properties of these phases are summarized in Table 1.1. Hot ionized gas is observed in X-ray emission and as UV absorption lines of highly ionized atoms (*e.g.*, C IV, N V, O VI). It is present in the coronal gas of stars and composes the Hot Ionized Medium (HIM), a hot and tenuous phase of the ISM. The gas in these regions is heated and ionized through shocks driven by stellar winds from early type stars and by supernova explosions. Diffuse ionized gas is observed mainly through emission in the Hα recombination line and resides in both a diffuse component, the so-called Warm Ionized Medium (WIM), as well as in the classical H II regions surrounding hot O and B stars. Neutral atomic gas is traced though the 21 cm line of atomic hydrogen, and is found in the Warm Neutral Medium (WNM) and Cold Neutral Medium (CNM). Molecular gas represents the densest component of the ISM. Although H_2 is the dominant molecular species in space followed by CO (H_2/CO = $10^4 - 10^5$), it cannot be routinely detected in cold gas by infrared telescopes because of the lack of dipole allowed transitions. Therefore, molecular gas is commonly traced through the CO rotational transitions, such as $J = 1-0$ at 2.6 mm. Molecular gas is localized in discrete Giant Molecular Clouds (GMC), which tend to be irregularly shaped with a density distribution far from homogeneous. Molecular clouds contain embedded cores in which new stars form.

Table 1.1 Main characteristics of interstellar medium components: coronal gas and hot ionized medium (HIM), H II regions, warm ionized medium (WIM), warm neutral medium (WNM), cold neutral medium (CNM), and molecular clouds. The values in this Table are taken from Tielens (2005) and Visser (2009).

Component	Fractional Volume (%)	Scale Height (pc)	Temperature (K)	Density (cm^{-3})	State of hydrogen
Coronal gas					
HIM	30–70	1000–3000	$10^6 - 10^7$	$10^{-4} - 10^{-2}$	ionized
WIM	20–50	1000	8000	0.2–0.5	ionized
H II regions	<1	70	8000	$10^2 - 10^4$	ionized
WNM	10–20	300–400	6000–10000	0.2–0.5	neutral atomic
CNM	1–5	100–300	50–100	20–50	neutral atomic
Molecular clouds	<1	70	10–50	$10^2 - 10^6$	molecular

1.2 The cycle of matter

The evolution of gas and dust in the ISM from stellar birth to death can be described as a cyclic event as shown in Fig. 1.1. The complete cycle takes some 2×10^9 years. In the first step, stellar winds and/or explosions enrich the diffuse interstellar medium in dust and gas. Carbonaceous dust grains are ejected by carbon-rich stars (C/O>1) at high densities and temperatures, and silicates originate from oxygen-rich star ejecta. Observations combined with models showed that $\lesssim$10% of the interstellar dust mass has a "stardust" origin (*i.e.*, formation in the atmospheres of evolved stars), and that interstellar grains are mostly formed in the ISM by some chemical mechanism which is not yet characterized (Draine 2009, and references therein). The interstellar grains pass through the various aforementioned phases of the interstellar medium several times on a typical scale of $\sim3\times10^7$ years, before they take part in the formation of a new star. In the intercloud phase, grains can coagulate leading to an increase in their size, while strong shocks destroy dust and change its size distribution. Supernova shocks can also trigger the collapse of diffuse clouds into dense clouds. In the denser phase, atomic gas is converted into simple molecules, like CO, through gas-phase reactions, while H-rich species such as H_2O, NH_3, and CH_4 are formed on the grains through surface reactions, resulting in a polar ice mantle. For densities higher than 10^5 cm^{-3} most of the gas-phase molecules, mainly CO, freeze-out onto the dust grains on timescales shorter than the lifetime of a core. The resulting apolar ice, which is typically a few tens of monolayers (ML) thick, is further involved in chemical reactions. The composition and evolution of interstellar ices are described in more detail in § 1.3.1.

Molecular clouds are stable over timescales of $\sim3\times10^7$ years because of a balance of turbulent and magnetic pressure and gravity. Physically this is expressed by the virial theorem, which states that, to maintain equilibrium, the gravitational potential energy must equal twice the internal thermal energy. The gravitational collapse of the core is initiated by the loss of turbulent or magnetic support. As it collapses, a molecular cloud can fragment into smaller pieces. Each of the cold cores collapses in an isothermal manner

since the gas (atoms and molecules) releases energy in the form of radiation (Bergin & Tafalla 2007). While the density increases (10^5–10^7 cm^{-3}), the fragments become optically opaque and are thus less efficient at releasing their energy through radiation. During the collapse the central cores (*i.e.*, the protostars) gradually warm up and emit a continuum of infrared radiation. The warm-up of cloud cores (20 K $< T <$ 100 K) induces the desorption of volatile species, like CO, O_2 and N_2, from dust grains and the segregation of less volatile ones, like CO_2. At such temperatures H atoms are no longer residing onto the grains, and therefore hydrogenation reactions are no longer a dominant process. Moreover, the increase in temperature facilitates a higher mobility of the solid species still frozen on the grains and, therefore, drives a rich grain-surface chemistry.

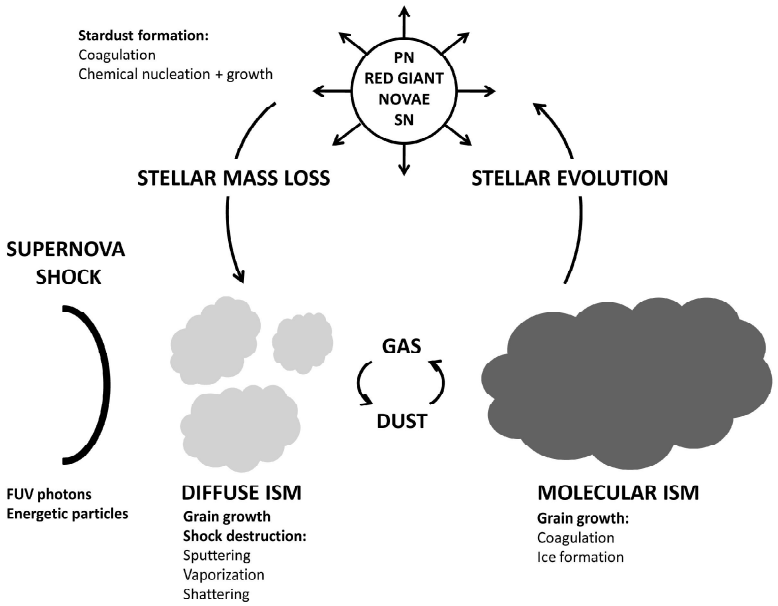

Figure 1.1 Schematic representation of the lifecycle of cosmic dust. Dust is formed in stellar ejecta (planetary nebulae, red giants, novae and supernovae) and mainly in the interstellar medium itself, where it cycles rapidly between the different phases. In the intercloud phase, strong shocks destroy dust and change its size distribution. In the denser phase, the accretion of gas-phase species onto grains forms an ice mantle, which is exposed to atoms and processed by FUV photons and energetic particles. Coagulation leads to an increase in the grain size. Ultimately, dust particles are involved in the star and planet formation process. Figure adapted from Tielens & Allamandola (1987b) and Tielens (2005).

The objects resulting from the cloud collapse are called Young Stellar Objects (YSOs). At this stage, YSOs are rotating spheres of gas with a central protostar. Stars of different

masses are thought to form by slightly different mechanisms. The process of single low- and intermediate-mass star formation ($M_\star < 8\ M_\odot$), schematically displayed in Fig. 1.2, is well understood (*e.g.*, Evans 1999, van Dishoeck 2004, and references therein). Because of the conservation of angular momentum the collapse of a rotating sphere of gas and dust (Fig. 1.2b) leads to the formation of an accretion disk through which matter is guided onto the central protostar (Fig. 1.2c). The temperature in the midplane of the disk drops to 10 K and the density increases to $\sim 10^{12}$ cm^{-3}. Therefore, gas-phase species will accrete onto the grains again. Also grains will coagulate, forming most likely larger and larger boulders, and eventually planets, even though this process is not completely understood yet. The surface of the disk is affected by a strong UV field from the protostar, the gas temperature often exceeds 100 K in the outer disk (>1000 K in the inner disk) and the density is $\sim 10^6$ cm^{-3}.

Under such harsh conditions, ices cannot survive and, therefore, only gas-phase species will participate in the chemistry of the warm inner envelope, known as hot core (Herbst & van Dishoeck 2009). Hot cores are characterized by a density of 10^7–10^8 cm^{-3}, a temperature of ~100 K and size of ~100 AU. Some excess angular momentum is also dissipated through large bipolar outflows, launched along the core's rotation axis near the protostar (Shu et al. 1991, Bally 2007). The gas present in the circumstellar disk will eventually fall onto the star, planets and small bodies present in the disk, or will be cleared by irradiation and winds from the star in a timescale of $\sim 10^6$ years (Fig. 1.2d-e). For low-mass stars, the disk will slowly evolve into a planetary system such as our Solar system (Fig. 1.2f). When the temperature of the protostar is sufficiently high to initiate nuclear burning of hydrogen into helium, a new star is born.

The formation process of high-mass stars ($M_\star > 8\ M_\odot$) is not yet fully understood because of observational problems: they are embedded objects that evolve rapidly to the main sequence. However, except for the most massive ones, massive stars most likely form by a mechanism similar to that observed for low-mass stars. It is likely that the initial phase involves the collapse of infrared dark clouds within giant clouds. High-mass young stellar objects are associated with ultra- or hypercompact H II regions, masers, outflows, and/or warm ambient gas at average temperatures of 300 K, known as hot cores (Herbst & van Dishoeck 2009). The hot cores usually have a size of 10^4 AU and often are associated with a rich organic chemistry. It is not yet clear whether disks are formed in high-mass star regions. If newly formed luminous O and B stars are in the proximity of cool interstellar matter, their UV radiation heats the neighboring gas and photodissociates molecules, producing heterogeneous Photon-Dominated Regions (PDRs) (van Dishoeck 2004).

Ongoing and future key new instrumentation, such as the *Herschel Space Observatory* and ALMA, will unravel the chemistry and dynamics of star and planet formation with more detail than possible so far. This will allow us to resolve the physical processes taking place during the collapse of molecular clouds, to image the structure of protostars and of protoplanetary disks, and to determine the chemical composition of the material from which future solar systems are made (van Dishoeck & Jørgensen 2008).

The final stages of the star evolution are well understood. Protostars with masses less than roughly 0.08 $M_\odot$ never reach temperatures high enough for nuclear fusion of

hydrogen to begin. These are known as brown dwarfs. For $0.08 < M_\star < 8\ M_\odot$, the star will spend a long time on the main-sequence phase (10^7–10^{10} yr) and nuclear fusion will form elements up to C, O and N. After leaving this phase, stars below 0.23 $M_\odot$ become white dwarfs, while more massive stars will move into the Red Giant and Asymptotic Giant Branch (RGB and AGB) phases and eventually evolve into a planetary nebula with a white dwarf core. Red giant winds and planetary nebulae are important sources of gas and dust enrichment in the ISM. In this way the matter cycle of low-mass stars is complete.

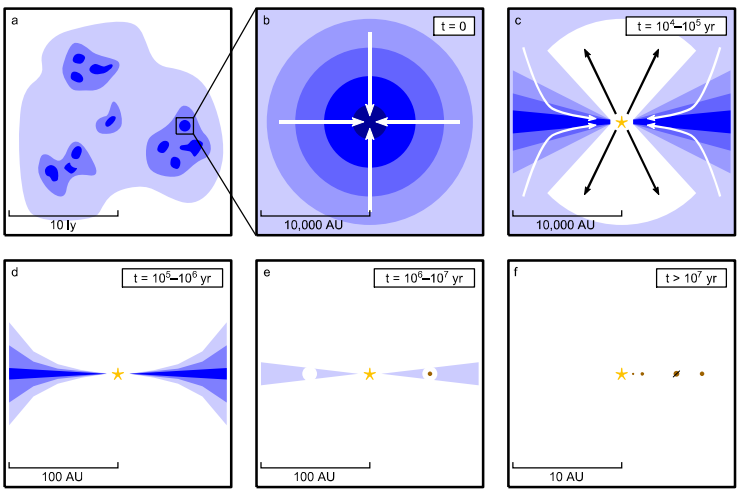

Figure 1.2 Schematic illustration of the different stages of low-mass star formation. Dense clouds can form when the diffuse medium is compressed by a shock event such as a supernova explosion (a). Once the density in the core of dense clouds gets high enough and support is lost, the core starts to collapse (b). Conservation of angular momentum results in the formation of a circumstellar disk and bipolar outflows (c). The disk will eventually evolve into a planetary system (d-f). Figure taken from Visser (2009), based on Hogerheijde (1998).

High-mass stars spend a shorter time along the evolutionary phases, burning elements up to Fe. Since no further energetically favorable nuclear reactions can occur, the core will collapse. Depending on the initial mass, the core can become a neutron star, a pulsar or a black hole. The outer shells of the star will explode in a violent event, a so-called supernova explosion, which can trigger the nucleosynthesis of elements heavier than Fe. These shocks can perturb the surrounding ISM and therefore trigger star formation closing the cycle of matter.

1.3 Interstellar ices

1.3.1 Interstellar ice composition

Rotational, vibrational, and electronic spectroscopy has established the presence of a large variety of polyatomic molecules, ions and radicals in space, both in the gas phase and in the solid state. In fact, over 150 different molecular species (excluding isotopomers) have been detected in the inter- and circumstellar medium. These species include a variety of inorganic compounds (*e.g.*, H_2O, CO, CO_2, NH_3, SO and SO_2), organics (*e.g.*, CH_4, H_2CO, CH_3OH, HCOOH, and CH_3CH_2OH), ions (*e.g.*, C_6H^-) and species identified only in the ice like OCN^- and NH_4^+), and unsaturated hydrocarbon chains (*e.g.*, HCN, HC_3N). Recently, large carbonaceous species like the fullerenes C_{60} and C_{70} have been unambiguously detected (Cami et al. 2010, Sellgren et al. 2010). However, aromatic species such as polycyclic aromatic hydrocarbons (PAHs) are not included in the count, since they are not uniquely identified. PAHs are detected only as a class through their infrared features. The spectra of molecular species are probes of the physical conditions and chemical history of the regions in space where they reside. Hence, high-resolution rotational and vibrational spectra improve our knowledge about the density and temperature of the gas as well as collapse of interstellar clouds, whereas vibrational spectra of solid phase molecules give information on the nature of the ice mantles covering dust grains.

The presence of ice in the interstellar medium was already proposed by Eddington (1937) before its spectral detection, which came almost four decades later: H_2O ice was detected at 3 μm by Gillett & Forrest (1973). Most ices can be detected in absorption in the mid-IR of an embedded object or along the line of sight of a background star. However, ground based observations in the mid-IR spectral window are limited because of telluric absorption. Airborne and space observatories have therefore been used to identify solid phase species in space in the last decades. In the 1990's the launch of the *Infrared Space Observatory* (ISO) revolutionized our understanding of interstellar ices. Because of its limited sensitivity, ISO observed mostly bright sources, such as high-mass YSOs and quiescent dense clouds toward luminous background stars (Gibb et al. 2000b, 2004). Observations show that H_2O, CO, CO_2, and, in some cases, CH_3OH represent the bulk of solid-state species in dense molecular clouds and star-forming regions. Minor ice components, such as CH_4, NH_3, H_2CO, HCOOH, SO_2, OCS, OCN^-, NH_4^+, and $HCOO^-$, are also observed, although their identification is sometimes controversial. Completely isolated single bands from species such as solid CH_4 at 7.67 μm and OCS at 4.92 μm are confidently assigned (see Table 1.2). However, the identification of other species like H_2CO, HCOOH and NH_3 is more problematic because all their strong vibrational modes overlap with features of other species (Table 1.2; van Dishoeck 2004, and references therein).

More recently, the *Spitzer Space Telescope* characterized the molecular content of icy grain mantles in the 5–35 μm wavelength range towards more than 40 low-mass protostars within the c2d (cores to disks) program (Boogert et al. 2008, Pontoppidan et al. 2008, Öberg et al. 2008, Bottinelli et al. 2010) and dozens more within other programs

Table 1.2 Interstellar ice inventory with respect to H_2O ice towards dark clouds, low- and high-mass YSOs. Selected solid state infrared transitions are also listed.

Species	Mode	λ (μm)	Dark cloud (Elias 16)	Low-mass YSO (HH 46)	High-mass YSO (W33A)
H_2O	O-H stretch	3.05	100	100	100
	H-O-H bend	6.0			
	libration	12			
CO	C=O stretch	4.67	26[a]	20[b]	8.1[c]
CO_2	C=O stretch	4.27	24[d]	21.6[e]	14.1[e]
	O=C=O bend	15.3			
HCOOH	C=O stretch	5.85	$\leq$1.4[f]	2.7[f]	5.2[f]
	CH deformation	7.25			
	C-O stretch	8.1			
H_2CO	C-H (asym., sym.)	3.47, 3.54	...	6.0[f]	3.1[c]
	C=O stretch	5.81			
	CH_2 scissor	6.69			
CH_3OH	O-H stretch	3.08	<2.3[f]	6.1[g]	14.7[f]
	C-H stretch	3.53			
	CH_3 deformation	6.85			
	CH_3 rock	8.85			
	C-O stretch	9.75			
NH_3	N-H stretch	2.96	$\leq$8[d]	6.1[g]	15[c]
	deformation	6.16			
	umbrella	9.0			
NH_4^+	deformation	6.85	5.2[f,i]	6.3[f,i]	8.1[f,i]
CH_4	C-H stretch	3.32	<3[d]	5.0[h]	1.5[c]
	deformation	7.67			
OCN^-	C$\equiv$N stretch	4.62	<2.3[d]	$\leq$0.6[j]	1.9[j]
OCS	O=C=S stretch	4.92	<0.27[c]	<0.04[k]	0.2[c]

[a]Chiar et al. (1995); [b]Boogert et al. (2004); [c]Gibb et al. (2004); [d]Knez et al. (2005); [e]Pontoppidan et al. (2008); [f]Boogert et al. (2008); [g]Bottinelli et al. (2010); [h]Öberg et al. (2008); [i]The entire band is assumed to be due to NH_4^+; [j]van Broekhuizen et al. (2005); [k]This value is taken from another low-mass YSO, Elias 29 (Gibb et al. 2004).

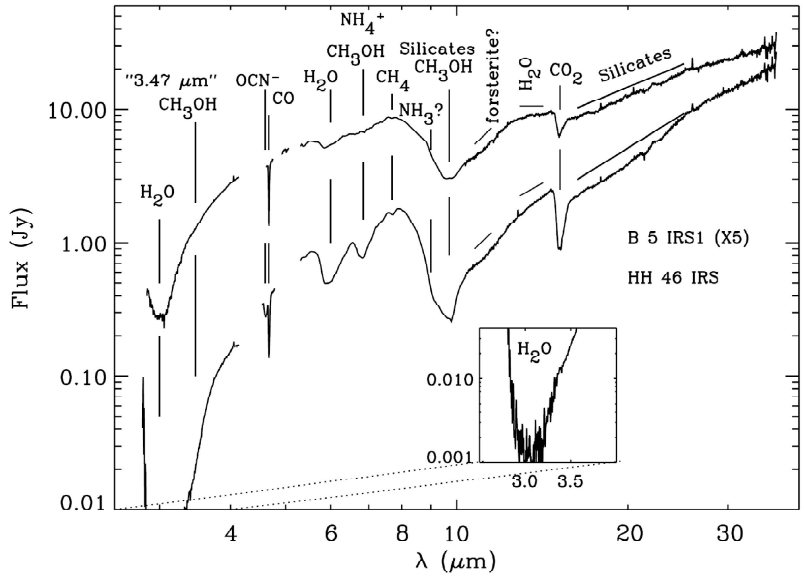

Figure 1.3 *Spitzer* infrared absorption spectrum combined with L and M band ground-based observations of two low-mass embedded stars: B5 IRS1 (*top, multiplied by a factor of 5 for clarification*) and HH46 IRS (*bottom*). Spectra taken from Boogert et al. (2004).

(*e.g.*, Zasowski et al. 2009). These data have been complemented with spectra at 2–4 μm obtained with ground-based facilities. These surveys provide the opportunity to unambiguously identify solid H_2O, CO_2, CH_4, CH_3OH, and NH_3. Figure 1.3 shows the *Spitzer* infrared absorption spectrum combined with L and M band observations of two low-mass embedded stars. In addition, *Spitzer* detected ices towards field stars behind quiescent dark clouds (*e.g.*, Bergin et al. 2005, Knez et al. 2005). Table 1.2 lists ice abundances with respect to H_2O ice towards high and low-mass protostars and quiescent dark clouds.

The general formation scenario can be summarized in four steps, as shown in Fig. 1.4.

1. In quiescent dark clouds, H_2O-rich ice is formed via surface reactions with a large amount of CO_2, and traces of CH_4 and NH_3 ice. Some CH_3OH is also associated with the H_2O-rich ice (Fig. 1.4a).

2. In the prestellar core, when densities are as high as 10^5 cm^{-3} and temperatures amount to ~10 K, CO and probably N_2 and O_2 molecules freeze-out on top of the H_2O-rich mantle, forming an apolar (water poor) ice layer. Before the turning-on of the protostar, a second CO_2 formation phase takes place resulting in a CO dominated CO:CO_2 ice mixture. During this phase, also CH_3OH ice is formed (Fig. 1.4b). Energetic processing, such as UV photolysis and cosmic rays irradiation, contributes to the production of new molecular species.

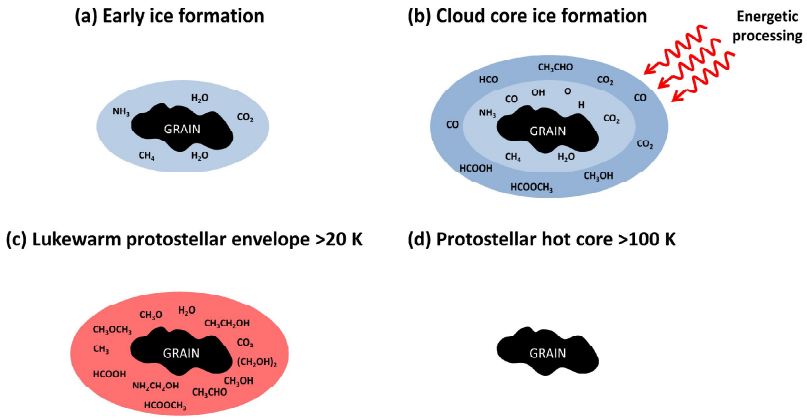

Figure 1.4 Suggested evolution of ices during star formation. Light-blue indicates a H_2O-dominated ice and dark-blue a CO-dominated ice. At each cold stage a small amount of the ice is released non-thermally. Early during cloud formation (a) a H_2O-rich ice forms. Once a critical density and temperature is reached CO freezes-out catastrophically (b), providing reactants for the formation of species like CH_3OH. Energetic processing (UV photolysis and cosmic rays irradiation) of the CO-rich ice results in the production of complex species. Closer to the protostar (c), following sublimation of CO, other complex molecules become abundant. Finally, all ice close to the protostar >100 K desorbs thermally (d). Figure adapted from Öberg et al. (2010a).

3. When the luminosity of the forming star increases, the more volatile species in the ice desorb, H_2O and CO_2 segregate, and more complex solid state chemistry is driven by the strong UV field coming from the young star (Fig. 1.4c).

4. When the temperature exceeds 90 K, the ice mantles evaporate completely and complex gas-phase chemistry can proceed in the hot cores (Fig. 1.4d).

The next section discusses the origin of the observed interstellar ices.

1.3.2 Interstellar ice chemistry

In quiescent dark clouds, grains provide a surface on which species can accrete, meet and react and to which they can donate excess energy. Grain surface chemistry is governed by the accretion rate of the gas phase species onto the grains, the surface migration rate, which sets the reaction network, and the desorption rate. The timescale at which gas phase species deplete-out onto grains is $\sim 10^5$ years in dense cores. This time is shorter than the lifetime of dense cores, which is between 10^5 and 10^6 years. Hence, in dense regions, during the first stage of star formation virtually all species (except H_2) are frozen-out onto interstellar grains.

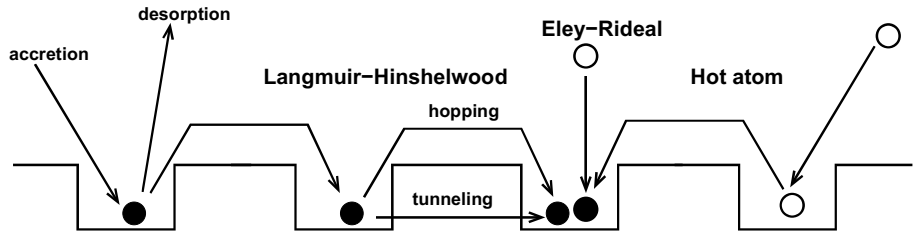

Figure 1.5 Three mechanisms for surface reactions on a regular grain surface: Langmuir-Hinshelwood (diffusive), Eley-Rideal, and hot atom mechanism. Closed circles are thermalized species and open circles non-thermalized. Reaction can occur when two species are in the same well. Figure provided by H. M. Cuppen.

As adsorbates accrete onto a cold surface, a complex chemistry occurs, leading to the production of new molecules in the ices through surface reactions (Herbst & van Dishoeck 2009, and references therein). There are three major mechanisms for surface reactions: Langmuir-Hinshelwood (diffusive), Eley-Rideal, and hot atom mechanism (see Fig. 1.5). In a Langmuir-Hinshelwood (LH) reaction the reactants are initially adsorbed onto the surface and in thermal equilibrium with the solid. Diffusion of one or more of the reactants on the surface leads to the formation of new products. In an Eley-Rideal (ER) reaction a particle coming from the gas phase reacts more or less directly with a surface-adsorbed species. In the hot atom mechanism, a gas-phase species lands on the surface and moves considerably before thermalization. In this way it is able to collide and react with an adsorbate.

In dense clouds, the flux of incoming species on a specific grain is typically very low ($\sim$1 per day). In contrast, on the grain surface, the abundant accreting atoms, H, C, N, and O, are relatively mobile and they can move around the grain on timescales less than the timescale for another gas phase species to accrete on the same grain. Moreover, the residence time of a species on a grain depends on its binding energy and grain temperature. As a result, for a 10 K grain with a site coverage of $\sim 10^6$ sites, an accreted H atom is expected to visit all sites on the surface many times before it desorbs. If co-reactants are present, H atoms can react before the next radical lands (Tielens & Charnley 1997, Tielens 2005). In considering possible co-reactants for atomic H, one has to distinguish between radicals and non-radicals. The former generally react with zero activation barriers; *i.e.*, upon collision on the grain surface. The latter may possess appreciable activation barriers, but, in each collision, there is a small probability that H will tunnel through the activation barrier and react. The reaction could also proceed thermally, depending on the residence time of both species (Herbst & van Dishoeck 2009).

Grain surface chemistry dates back to Allen & Robinson (1977), although the first realistic gas-grain model was proposed by Tielens & Hagen (1982) in 1982. Their astrochemical model includes a complex grain surface reaction network to explain molecule formation in quiescent dark clouds. According to this model in a first phase, H_2O ice (the dominant solid phase species) can be produced by the sequential hydrogenation of

O atoms landing on the grain (a process first proposed by van de Hulst; for a review see van de Hulst 1996). Atomic oxygen can also react with other O atoms to form O_2 and O_3. Reaction of O_3 with H reforms O_2 and OH. O_2 can be hydrogenated to form H_2O, while the OH radical can react with H or H_2 to form again H_2O, or it can form CO_2 and H_2 with the CO accreted on the surface. Under these conditions, also other H-rich species such as CH_4 and NH_3 can be formed. This first phase of grain-surface chemistry results in the formation of a polar ice mantle (water-rich) onto the dust grains. During the second phase, when the density increases in the molecular cloud, CO freezes-out onto the grains (its accretion rate is higher than that of H) forming an apolar ice layer (water-poor) on top of the polar one. Under these conditions, the hydrogenation of CO ice can lead to the formation of H_2CO and CH_3OH (Tielens & Hagen 1982, Charnley et al. 1997). CO_2 can be formed through the reaction CO + OH (Goumans et al. 2008). As suggested by Charnley et al. (2001), the reaction between CO and heavier elements than H may lead to the formation of more complex molecules such as CH_3COH and C_2H_5OH.

All these astrochemical reaction networks were based on chemical intuition and analogues from gas phase routes. It took several decades before experimental techniques allowed laboratory astrochemists to put all these reactions to the test. This is now done by several groups across the world and is the main topic of this thesis (Chapters 2-8). In this experimental process, several of these reactions were proven to be efficient, whereas others were not. Also several new reaction routes were revealed. Thus, laboratory work combined with theoretical models plays an essential role in disentangling the astrochemistry of the ISM.

The mathematical treatment of grain-surface reactions is not straightforward because of the heterogeneity and small size of the grains (Herbst & van Dishoeck 2009). Rate equations[1] are better used to reproduce the diffusive chemistry on homogeneous larger grains, on which at least several reactive adsorbate species exist on average (Green et al. 2001, Tielens & Hagen 1982). So-called macroscopic stochastic methods such as the master equation approach[2] and the Monte Carlo method [3] eliminate the problem caused by the small numbers of adsorbates, which is significant on smaller grains, but do not solve the problem of inhomogeneity (Barzel & Biham 2007, Charnley 2001, Green et al. 2001, Stantcheva et al. 2002). A special Monte Carlo method known as the "continuous-time, random-walk" approach handles this latter problem (Chang et al. 2007). This Monte Carlo method follows the species on the surface of the grain; explicitly takes into account processes, such as accretion, hopping, reaction, and desorption; takes into account the layering, investigating the penetration of species into the ice; and is a stochastic approach.

Several of these mathematical methods are implemented in Chapters 2 and 3. In Chapter 2, for instance, a Monte Carlo approach is used to simulate CO hydrogenation under laboratory conditions. Cuppen et al. (2009) extended this model using the continuous-

[1]Rate equations are differential equations which link the reaction rate for a chemical reaction with concentrations of reactants and constant parameters (like rate coefficients and partial reaction orders).

[2]The master equation is a set of first-order differential equations describing the time evolution of the probability of a system to occupy each one of a discrete set of states.

[3]The Monte Carlo method is based on a class of computational algorithms that rely on repeated random sampling to compute their results.

time, random-walk Monte Carlo method in order to simulate microscopic grain-surface chemistry over the long timescales in interstellar space, including the layering of ices during CO freeze-out. In Chapter 3, reaction rates are obtained by fitting a set of differential equations to the time evolution experimental curves of newly formed H_2O (D_2O) and H_2O_2 (D_2O_2) through O_2 hydrogenation (deuteration).

Surface reactions between thermalized reactants are not the only mechanism leading to the formation of new molecular species in the solid phase. Interstellar ices undergo energetic processing due to cosmic ions and UV photons, which may induce non-thermal desorption of surface molecules as well as the production of complex species. Fast ions passing through molecular solids release their energy into the target material. As a consequence, many molecular bonds are broken along the ion-track and, in a short time (less than one picosec), the molecular fragments recombine to produce a rearrangement of the chemical structure that leads to the formation of new molecular species. In the case of UV photolysis, the energy is released into the target material by a single photodissociation or photoexcitation event. In this particular case, new molecular species are also formed. Energetic processing, thus, offers a complementary pathway to atomic addition reactions towards chemical complexity in space (*e.g.*, Hagen et al. 1979, Gerakines et al. 1995, Hudson & Moore 2000, Palumbo et al. 2008, Chapter 9). This thesis shows that, for instance, the total observed abundance of molecules like CO_2 can be formed in the solid phase through surface reactions without energetic input (Chapter 7) as well as through energetic processing of C- and O- bearing molecules that induces surface chemistry (Chapter 9). Recent models supported by laboratory studies show that UV photolysis and ion irradiation of simple ices, such as CH_3OH, NH_3, and CH_4, trigger a complex surface chemistry. The desorption of these products in the warm inner regions of protostellar envelopes may explain the observed gas-phase abundances of complex organic molecules in such environments (*e.g.*, Garrod et al. 2008, Öberg et al. 2009b, Modica & Palumbo 2010).

1.4 Laboratory ices

Laboratory setups that record vibrational spectra of ices typically consist of a radiation source, a sample chamber, and an instrument for spectra acquisition. These elements are also present in space: the radiation source is a field star or an embedded source, the sample chamber is the interstellar medium, with dust grains as the surface, and the recording instrument is the spectrograph mounted onto the telescope. The interpretation of ice data is achieved by studying interstellar ice analogues in the laboratory spectroscopically and comparing spectra directly to astronomical observations. Spectra acquired in transmission[4] provide information on the ice constituents in space, their corresponding mixing ratios, ice structure and temperature. From such a comparison it was found that dust grains in cold (<100 K) and dense interstellar environments are covered by 50−100 monolayers thick icy mantles, which comprise primarily H_2O, but also other species, like CO, CO_2,

[4]The IR light passes through the icy sample, which is deposited onto a cold (10−300 K) infrared transparent window (CsI, Si or KBr) and then detected by an infrared spectrometer.

CH_3OH, HCOOH, NH_3, CH_4, and traces of more complex molecules. These ices are mainly amorphous and have a layered structure consisting of H_2O- and CO-dominated ice mixtures, as discussed in §1.3.1. Spectroscopic ice work is still ongoing, even after more than 30 years of dedicated work. Recent examples comprise work performed in the Sackler Laboratory for Astrophysics in Leiden on the effect of CO_2 and CO on H_2O band profiles and band strengths by Öberg et al. (2007a) and Bouwman et al. (2007), respectively. Figure 1.6 shows infrared spectra in transmittance of the four H_2O band modes, ranging between 4000 cm^{-1} and 500 cm^{-1}, for six different ice compositions: from pure H_2O ice (*bottom panels*) to a H_2O:CO = 1:4 mixture (*top panels*) (Bouwman et al. 2007). For different mixture ratios the shape and peak position of the absorption bands vary. This allows to use the laboratory data to conclude on ice parameters in the ISM.

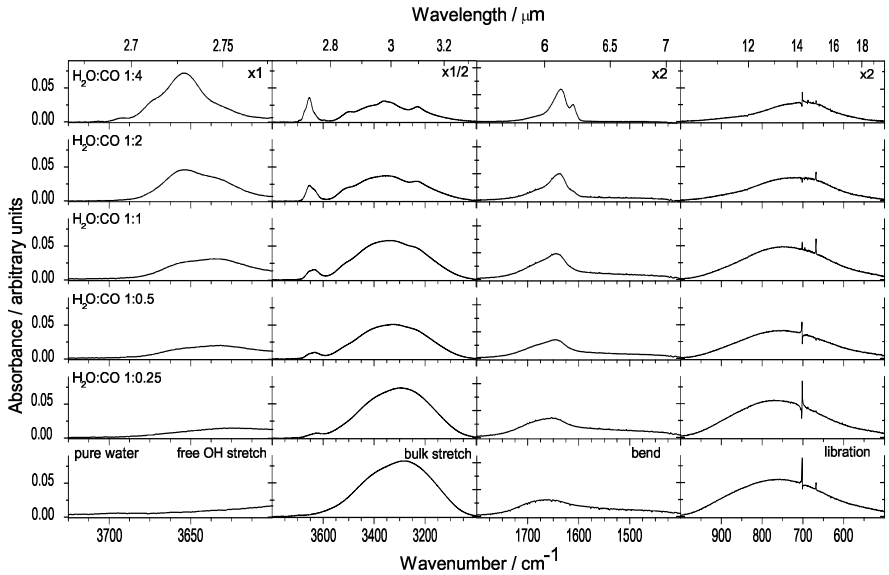

Figure 1.6 The 15 K infrared absorption spectra in transmittance of the four H_2O band modes between 4000 cm^{-1} and 500 cm^{-1} for six different ice compositions, ranging from pure water ice (*bottom panels*) to a H_2O:CO = 1:4 mixture (*top panels*). For different mixture ratios the shape and peak position of the absorption bands vary. Note that the wavelength ranges for separate modes are different. The small structures on the libration mode are experimental artifacts. Spectra are taken from Bouwman et al. (2007).

The experimental setup used for these measurements consists of a High Vacuum (HV) setup in which ices are grown onto a cold infrared-transmitting window (10–300 K). The window is cooled down by a closed-cycle He refrigerator and the sample temperature is controlled by resistive heating. A Fourier transform infrared (FTIR) spectrometer is used to record the ice spectra in transmission between 4000–400 cm^{-1} (2.5–25 μm) with a typical resolution of 1–2 cm^{-1}. This allows a straightforward detection in a single pass

experiment. The main weakness of this method is that the base pressure in the main chamber is 1×10^{-8}–1×10^{-7} mbar, which is orders of magnitude higher than the densest interstellar cloud, and water pollution is not negligible (>100 ML of H_2O deposited per hour on a 10 K substrate), since the vacuum is mainly composed by background H_2O. In order to minimize these effects, experiments are performed in a short timescale (~few hours) and thick layers of ice are usually deposited on the substrate (>0.1 μm).

The formation of complex species through energetic processing (ions and UV photons) of simple ices have been experimentally investigated for decades using HV setups (*e.g.*, Hagen et al. 1979, Allamandola et al. 1988, Gerakines et al. 1995, Hudson & Moore 2000, Strazzulla & Palumbo 2001, Mennella et al. 2004, Mennella et al. 2006, Bennett & Kaiser 2007, Palumbo et al. 2008, Chapter 9). With few exceptions, these experiments are meant to investigate qualitatively and, more recently, quantitatively the effect of energetic processing on the interstellar chemistry, with the intent to mimic ice composition in star forming regions. The work presented in Chapter 9 is performed in a HV system and a quantitative comparison between laboratory and observational infrared spectra is made. In this chapter the interstellar ice analogs are obtained in situ upon ion irradiation of selected ice samples.

Another main objective of laboratory work is the characterization of astrophysically relevant ice processes, such as surface formation, diffusion, segregation, and thermal and non-thermal desorption of molecules. The investigation of these ice processes started only roughly a decade ago with the introduction of a new generation of systems derived from standard surface science techniques, called Ultra High Vacuum (UHV) setups (1×10^{-10}–1×10^{-11} mbar). The gas composition in UHV setups reproduces the interstellar environment in the sense that it is mainly composed of H_2 with densities comparable to the disk midplane. The surface temperatures reached in these chambers are as low as <10 K. The water contamination rate on a 10 K substrate is <1 ML per 3 hours. Two UHV surface techniques are used as analytical tools: Reflection-Absorption InfraRed Spectroscopy (RAIRS) to investigate species in the solid phase, and Temperature Programmed Desorption (TPD) using a Quadrupole Mass Spectrometer (QMS) in order to monitor gas-phase species desorbed from the ice.

Although the importance of surface reactions for interstellar chemistry was already realized in the 1940s, the surface formation of complex molecules in interstellar ice analogs has only been investigated recently by atomic addition experiments (*e.g.*, Hiraoka et al. 1998, Watanabe et al. 2006a, Matar et al. 2008, Chapters 2-8). Most of the laboratory work so far focuses on the hydrogenation/deuteration of simple ices such as CO, O_2, and O_3 (*e.g.*, Chapters 2-6 and references therein; see Fig. 1.7). In Chapters 7-8 the hydrogenation of CO:O_2 binary mixtures is presented. Chapter 7 focuses on the formation of solid CO_2 through direct dissociation of the HO-CO complex. This chapter investigates at the same time the competition between the different hydrogenation channels (CO + H vs. O_2 + H), while Chapter 8 focuses on the formation of HCOOH ice through the hydrogenation of the HO-CO complex. Neither the surface formation of CO_2 nor that of HCOOH have been observed in hydrogenation experiments of pure CO and O_2 ices. The experiments presented in all these chapters are not designed to simulate a realistic interstellar ice, but to test surface reaction pathways. So far few studies have investigated the

hydrogenation of more complex species, such as CO_2, HCOOH, and CH_3CHO containing ices (Bisschop et al. 2007b), or focused on the bombardment of simple ices with heavier species than hydrogen/deuterium atoms, using a single or a double beam line (*e.g.*, Oba et al. 2010, Dulieu et al. 2010).

UHV setups have been recently used to investigate UV induced ice chemistry. Also in this case experimental results are not meant to be directly compared to astronomical observations. Rather a synergic use of RAIRS and TPD is meant to study the physical properties of the ice. Examples are the systematic investigation of photodesorption of simple molecules, such as CO, N_2, H_2O and D_2O, as well as the study of photochemistry in CH_3OH-rich ices and H_2O:CO_2:NH_3:CH_4 mixtures (*e.g.*, Öberg et al. 2007b, 2009d,c,b, 2010b).

1.4.1 RAIR spectroscopy

The main advantage of the RAIRS detection technique is that the reactants and products are monitored in the solid phase at the time and temperature of interest. Figure 1.7 shows the RAIR spectra from a CO hydrogenation experiment, as presented in Chapter 2. The top panel of Fig. 1.7 shows the 15 K CO ice spectrum after deposition, while the bottom panel shows the RAIR difference spectra with respect to the initial deposited ice acquired during H-atom exposure. Quantifying the formed product with the RAIRS technique is relatively simple, provided that the RAIRS is calibrated with an independent method, even though, not all species can be detected in the infrared[5]. The column densities of reactants and products are usually obtained from the integrated intensity of the selected infrared bands, using a modified Lambert-Beer equation (Bennett et al. 2004):

$$N_X = \frac{\int A(\nu)\mathrm{d}\nu}{S_X} \tag{1.1}$$

where $A(\nu)$ is the integrated absorbance and S_X is the corresponding band strength for species X (see Chapter 2 and 4). Since literature values of transmission band strengths cannot be used directly in reflectance measurements, an apparent absorption strength of the various species is obtained from calibration experiments. The determination of this apparent absorption strength is set-up specific. The calibration method (isothermal desorption of a selected ice) is described in detail in Chapters 2 and 4.

The RAIR technique has both advantages and disadvantages over transmission infrared spectroscopy. Since RAIRS is performed in a grazing incidence configuration with respect to the substrate, which is often a copper plate covered by a film of polycrystalline gold[6], the resulting enhancement of the p-polarized electric field at the surface leads to a sensitivity advantage. Furthermore, in the reflection mode a double-pass geometry is used. The incident beam must pass once through the surface layer before hitting the reflecting substrate, and a second time on its way to the detector. The adoption of a grazing

[5]Diatomic homonuclear molecules like O_2 and N_2 are infrared in-active, except when embedded in an ice matrix (Ehrenfreund et al. 1992).

[6]The gold substrate is chemically inert, *i.e.*, it does not have a direct effect on the behavior of the ice.

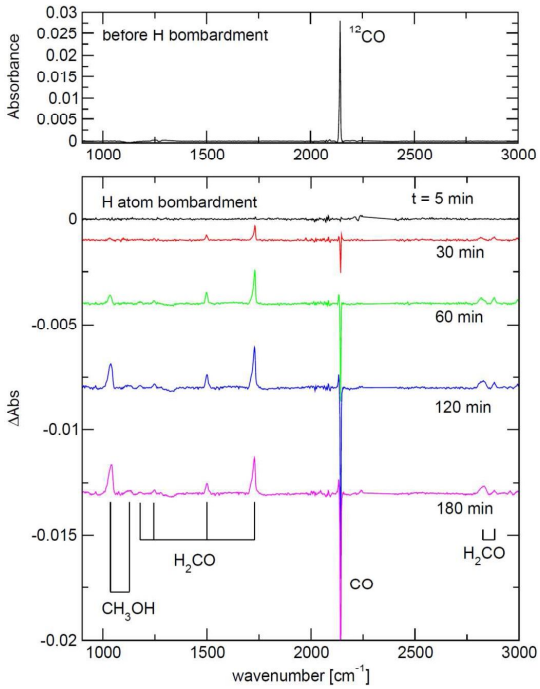

Figure 1.7 The RAIR spectra of a CO hydrogenation experiment taken from Chapter 2. The top-panel shows the CO ice spectrum at T = 15 K. The bottom panel shows the RAIR difference spectra with respect to the initial deposited ice acquired during H-atom exposure.

incidence geometry also leads to a rapid increase in path length, hence increasing the sensitivity for very thin ice layers. Thus, in a surface analysis experiment, RAIRS can probe ice layers down to the monolayer regime and therefore it can be considered a more sensitive technique than transmission infrared spectroscopy. However, the main disadvantage is that RAIR spectra cannot be directly compared to astronomical spectra. Therefore, as previously mentioned, experiments using RAIRS are often not meant to reproduce interstellar ice analogs, but to investigate interstellar relevant solid state processes. Moreover, the RAIRS detection technique is often complimented by the TPD technique for these kind of experiments of which Chapters 2 and 8 are two examples. In the experiments shown in these two chapters, after H-atom addition a TPD experiment is performed and gas-phase molecules are detected by a QMS. The combination of the two techniques led to the unambiguous identification of surface CH_3OH and HCOOH formation at low temperatures, respectively.

1.4.2 Mass spectrometry

As discussed in the first part of this chapter, in the earliest stages of star formation virtually all species (excluding H_2) accrete onto grains in dense cold cores. In the later stages, grains are warmed to temperatures where molecules desorb into the gas phase. Thus, the less volatile species will still reside on the grain surface and participate in reactions in the solid state, until the grain temperature will exceed 90 K, at which the entire interstellar ice mantle is desorbed. This scenario, which takes place at astrophysical timescales of $\sim 10^7$ years, can be experimentally simulated on laboratory timescales of a few hours through a TPD experiment. An ice sample is prepared under UHV conditions with monolayer precision and heated linearly with a selected rate (*e.g.*, Fraser et al. 2001, Collings et al. 2003, 2004, Bisschop et al. 2006, Acharyya et al. 2007). The desorbed species are subsequently recorded as a function of temperature using a QMS, which produces a signal proportional to the number of incoming molecules as a function of their mass to charge ratio (m/z). The incoming molecules first enter the ion source of the QMS, where they are ionized through electron bombardment by electrons released from a hot filament. The resulting ions are then focussed, selected and directed to the detector. Ions are detected by a Faraday detector, which collects the ions directly, allowing the ion current to be monitored. Alternatively, for higher sensitivity, a Channel Electron Multiplier (CEM) can be used. This type of detector is a Secondary Electron Multiplier (SEM) in which a large negative potential ($\sim$ - 2000 V) is used to attract the ions into the channel entrance. The channel is coated with a material that readily releases secondary electrons upon ion/electron impact. This produces a cascade of electrons down to the channel which can be detected, either as the electron current, or as a series of pulses.

Whilst the TPD experiment itself is relatively straightforward, the interpretation of the data is often much more challenging. Under conditions where the pumping speed is sufficiently high, the QMS signal for the selected mass is proportional to the rate of desorption of that species, r_d (molecules cm^{-2} s^{-1}). The rate of desorption is given by the Polanyi-Wigner equation:

$$r_\mathrm{d} = \nu_i N_X \exp(-E_\mathrm{d}/RT) \tag{1.2}$$

where ν_i is the pre-exponential factor for the process leading to the desorption, N_X is the surface concentration of adsorbate X, i is the desorption order, E_d is the activation energy for desorption per mole, R is the gas constant and T the temperature. Desorption from multilayers of bulk ice is typically close to zero order ($i = 0$). For perfect zero order desorption, the desorption rate does not depend on the surface concentration. In many cases, desorption of submonolayer coverage results in near first order kinetics ($i = 1$), *i.e.*, indicating that the desorption rate depends linearly on the surface concentration. This two desorption regimes can be experimentally investigated performing an isothermal desorption experiment, as shown in several chapters of this thesis.

The simplest thermal desorption process is the desorption of a pure ice. Desorption of binary or more complex mixtures is less understood. Figure 1.8 shows the TPD curves for CO and CO_2 desorption from pure ice (*solid lines*) and mixed with water (*dotted*

lines) (Öberg 2009). The desorption energy of the single species depends on the exact ice composition. In addition, the dominant mantle species may prevent other species from desorbing. Molecules can, indeed, get trapped in the matrix and then be released at different temperatures than their thermal desorption temperatures. Laboratory experiments show that ice heating also results in ice segregation of previously mixed ices (*e.g.*, Öberg et al. 2009a, Chapter 9).

Although, TPD is a more sensitive technique than RAIRS, it has however several disadvantages: the surface reaction products, which remain in the solid phase, cannot be probed in situ; additional surface reactions during the TPD (during the linear heating of the ice and before complete desorption of the species) cannot be excluded; quantifying the desorbing species is not straightforward; and some of the interesting species have equal (*i.e.*, undistinguishable) masses or are fractionated in the QMS upon electronic bombardment. A TPD experiment finally destroys the ice.

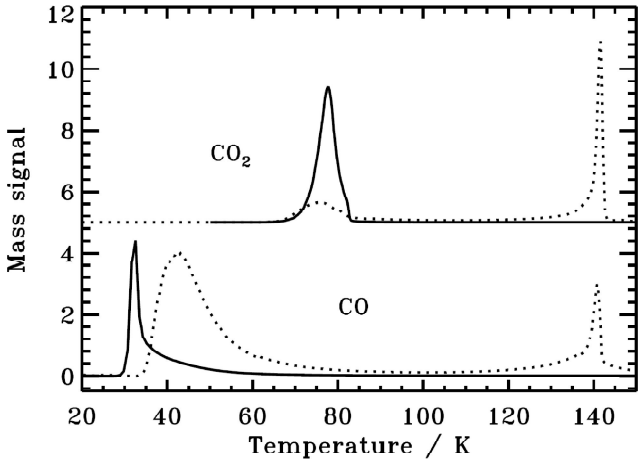

Figure 1.8 TPD curves for CO and CO_2 desorption from pure ice (*solid lines*) and H_2O:CO = 5:1 and H_2O:CO_2 = 4:1 (*dotted lines*) binary mixtures. The TPD spectra are normalized with arbitrary factors for visibility and are taken from Öberg (2009).

1.4.3 Experimental setups used in this thesis

SURFRESIDE

Chapters 2-8 are dedicated to the investigation of surface reactions that can lead to the formation of interstellar relevant molecules. All experiments are performed in the Sackler laboratory for Astrophysics using an UHV setup SURFace REaction SImulation DEvice

(SURFRESIDE), which consists of a stainless steel vacuum main chamber and an atomic line. A schematic view of the experimental apparatus is shown in Fig. 1.9. The gold coated copper substrate temperature is controlled between 12 and 300 K. Deposition of selected gasses proceeds under an angle of 45°, with a controllable flow. Gas phase molecules are monitored during the deposition mass spectrometrically by means of a QMS, which is placed behind the substrate and opposite to the atomic source. A thermal cracking source (Tschersich & von Bonin 1998, Tschersich 2000, Tschersich et al. 2008) is used to hydrogenate the ice sample through heating a capillary pipe, in which H_2 flows, from 300 to 2250 K by a surrounding tungsten filament. A quartz pipe is placed along the path of the dissociated beam to efficiently thermalize all H atoms to room temperature through surface collisions before they reach the ice sample. The Hydrogen Atom Beam Source (HABS) atom fluxes are measured at the substrate position mass spectrometrically, as described in the appendix of Chapter 4.

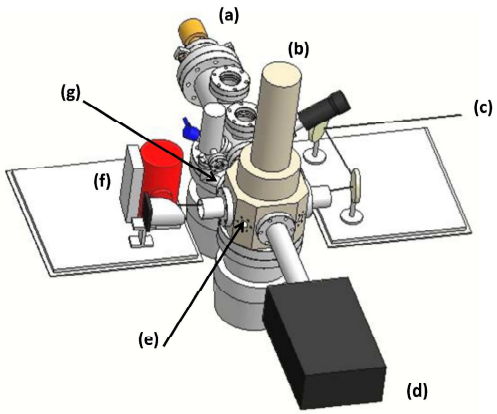

Figure 1.9 Schematic top-view of the solid-state experimental UHV set-up (SURFRESIDE): $^{(a)}$H-atom source; $^{(b)}$cold finger; $^{(c)}$IR beam; $^{(d)}$mass spectrometer; $^{(e)}$main chamber; $^{(f)}$IR detector; $^{(g)}$deposition line.

Ices are monitored by means of RAIRS using a FTIR spectrometer, which covers the range between 4000 and 700 cm^{-1} (2.5–14 μm). A spectral resolution between 1 and 4 cm^{-1} is used and several scans are co-added. In Chapters 2-4 and 6-7, the ice is first deposited and then hydrogenated/deuterated. In this case, RAIR difference spectra with respect to the initial deposited ice are acquired during H/D exposure. In Chapters 5 and 8, molecules are co-deposited with H atoms and RAIR difference spectra with respect to the bare substrate are acquired during co-deposition. In all cases, newly formed solid species are monitored by RAIRS. Spectra are recorded at different stages during an experiment, providing time resolved information about the destruction (*i.e.*, use-up) of the precursor ice (the deposited ice layer) and the formation of new molecules that are identified through their spectral fingerprints. At the end of the atomic addition a TPD can be performed to constrain the experimental results. Surface reactions of simple ices, like CO, O_2, O_3, and

$CO:O_2$ mixtures are investigated during a full range of laboratory conditions including different atomic fluxes, ice temperatures, ice thicknesses, ice structures, and mixture ratios with the intent to unreveal the physics and chemistry of molecule formation more than simulating chemistry in a realistic interstellar ice. However, in Chapter 3 also the astronomical implications of H_2O formation are examined in more detail.

HV setup in LASp

The experiments discussed in Chapter 9 are performed in the Laboratory for Experimental Astrophysics (Laboratorio di Astrofisica Sperimentale - LASp) in Catania (Italy). The experimental setup used to obtain infrared transmission spectra is composed of a stainless steel HV chamber interfaced with a FTIR spectrometer (4400−400 cm^{-1}) comparable to the setup described in § 1.4. Molecules are injected into the chamber through a needle valve and subsequently deposited onto a chosen substrate (Si or KBr) placed in thermal contact with a cold finger (10−300 K). After deposition the samples are bombarded by 200 keV H^+ ions. The ions are obtained from an ion implanter interfaced with the vacuum chamber. The used beam produces current densities in the range from 100 nA cm^{-2} up to a few μA cm^{-2} in order to avoid macroscopic heating of the target. The ion beam and the infrared beam are mutually perpendicular, forming an angle of 45° with the substrate plane. In this way, spectra can be taken at any time of the experiment without tilting the sample. The energy released to the sample by impinging ions (dose) is given in eV/16 u, where u is the unified atomic mass unit defined as 1/12 of the mass of an isolated atom of carbon-12. The polarization of the infrared radiation is selected by rotating a polarizer placed in the infrared beam path before the detector. Therefore, for each single irradiation-step two spectra are acquired in different polarizations: one with the electric vector parallel (P polarized) and one perpendicular (S polarized) to the plane of incidence.

1.5 This thesis

Chapter 2

Chapter 2 focuses on the formation of formaldehyde (H_2CO) and methanol (CH_3OH) by hydrogenation of pure CO ice. Reaction rates are determined from RAIR data for different ice temperatures and ice thicknesses, as well as H-atom fluxes (1×10^{12}−2.5×10^{13} H atoms cm^{-2} s^{-1}). The formation of new molecules in the ice is confirmed by TPD: H_2CO and CH_3OH are also found mass spectrometrically. On the basis of these experiments energy barriers for the H + CO and H + H_2CO reactions are obtained by fitting Monte Carlo simulation results to the experimental data. Using these barriers, the CH_3OH production can be simulated for interstellar conditions (Cuppen et al. 2009) and from this work, surface hydrogenation of CO ice can now be safely used to explain the observed abundance of CH_3OH in the interstellar medium.

Chapters 3-6

Water ice formation through surface reactions is extensively discussed here. In 1982 Tielens & Hagen (1982) proposed that interstellar water forms on grain surfaces through three reaction channels: hydrogenation of atomic oxygen, molecular oxygen and ozone. In Chapter 3, the molecular oxygen channel is investigated for a large range of temperatures. The main and surprising finding is that the initial formation rate of H_2O_2 and H_2O is much less temperature dependent than the analogous reactions for CO hydrogenation. Furthermore, O_2 hydrogenation results in a much larger yield than the few monolayers found for CO hydrogenation. This yield is strongly temperature dependent. In Chapter 4, both effects are shown to be a direct consequence of the competition between the reaction of H atoms with O_2 molecules, which is barrierless and therefore temperature independent, and the H-atom diffusion into the O_2 ice, which is temperature dependent. In Chapter 4, O_2 hydrogenation is investigated extensively from a physical approach, *i.e.*, studying different ice thicknesses, ice temperatures, ice structures and H_2 concentrations in the atomic beam, whereas Chapter 5 focuses more on the reaction scheme with the intent to assess reaction routes and branching ratios. The latter Chapter shows that the initially proposed reaction network of only three channels is too simple and that several of the channels are actually linked through additional reactions.

The hydrogenation of solid O_3 is discussed in Chapter 6. Since this channel is connected to the O_2 channel after the first reaction step, special care is taken in Chapter 6 to deposit a pure O_3 ice (free from O_2 contamination[7]) by keeping the substrate temperature between the O_2 and O_3 desorption temperature during deposition. If such a temperature is also kept during H-atom addition, the O_2 molecules formed upon O_3 hydrogenation will desorb from the surface of the ice. Thus, in this way the reaction of OH to form water by reaction with H or H_2 can be investigated. The hydrogenation of O_3 is found to be more similar to CO hydrogenation in the sense that only the top few monolayers of O_3 are hydrogenated. Moreover, the reaction OH + H_2 could be more efficient than the reaction OH + H: reaction OH + H_2 could proceed through tunneling, while reaction OH + H needs to dissipate 5.3 eV of excess energy with just one final product, which could be difficult. The conclusion that the three channels ($O/O_2/O_3$ + H) are strongly linked, is of importance for astrochemical models focusing on water formation under interstellar conditions.

Chapter 7

Chapter 7 discusses the hydrogenation of CO:O_2 binary mixtures, which results in the formation of CO_2 through the reaction of OH and CO. Surface CO_2 formation without energetic input is found to be an important formation mechanism, which may explain the formation of CO_2 together with H_2O ice during the dense cold core phase prior to star formation. The competition between CO hydrogenation and O_2 hydrogenation reveals that the penetration depth of H atoms into the ice depends strongly on the ice composition,

[7]Some gas phase O_2 can be formed in the deposition line and in the main chamber through O_3 dissociation.

and that the CO and O_2 channels influence each others final product yields. However, the formation rate for all the final products is found to be less sensitive on the mixture composition than the final yield. Therefore, the formation rates found for H_2CO, CH_3OH, H_2O_2 and H_2O in the isolated studies of the CO + H (Chapter 2) and O_2 + H (Chapter 3) channels are valid for use in astrochemical models.

Chapter 8

Chapter 8 deals with the formation of solid formic acid (HCOOH). The aim of Chapter 8 is to give the first experimental evidence for solid HCOOH formation at low temperature through the hydrogenation of the HO-CO complex, stabilized in the ice by intramolecular energy transfer to the surface, as proposed by Goumans et al. (2008). Formation of HCOOH is observed in the infrared after co-deposition of CO:O_2 mixtures and H atoms, increasing the ice temperature below the CO and O_2 desorption temperature (<30 K) and therefore increasing the mobility of the ice components only. At these temperatures H atoms, trapped in the ice matrix or formed through surface reactions, can find and react with the stabilized HO-CO complex. These experiments demonstrate that the reaction HCO + OH is inefficient at low temperatures. In the last part of the chapter, experimental results are placed in an astrophysical context. It is shown that the HO-CO complex channel, which was previously not considered as an important HCOOH formation route, explains the presence of HCOOH in dense cold clouds, at the beginning of the warm-up phase of a protostar.

Chapter 9

Chapter 9 discusses the formation of solid CO_2 through reactions induced by energetic processing of C- and O- bearing molecules. Chemical and structural modifications of the interstellar ice analog samples induced by energetic processing are analyzed using infrared spectroscopy in transmittance. Therefore, a quantitative study is obtained with the intent to compare laboratory results to observations. Experiments show that laboratory spectra are a good spectroscopic analogue of the interstellar features. Even if the comparison between laboratory and observed spectra presented here cannot be considered unique and complete, our results quantitatively show that interstellar solid CO_2 can form after ion irradiation and UV photolysis of icy mantles. The results presented here complement those shown in Chapter 7, where the CO_2 formation without energetic input is investigated. Both mechanisms can, indeed, contribute to the total CO_2 column density observed in quiescent clouds and star forming regions.